

Tunable liquid crystal Fabry-Perot hyperspectral imaging detectors in mid-infrared

Fu Anbang^{1,2,3}, Zhang Huaidong^{1,2,3}, Zhang Xinyu^{1,2,3}, Sang Hongshi^{1,2}, Ji An⁴, Xie Changsheng^{1,2,3}

- (1. National Key Laboratory of Science & Technology on Multispectral Information Processing, Wuhan 430074, China;
2. Institute for Pattern Recognition and Artificial Intelligence, Wuhan 430074, China;
3. Wuhan National Laboratory for Optoelectronics, Huazhong University of Science Technology, Wuhan 430074, China;
4. Institute of Semiconductors, The Chinese Academy of Sciences, Beijing 100083, China)

Abstract: This paper proposed a novel method for investigating the characteristics of an electrically tunable liquid crystal(LC) Fabry-Perot(FP) hyperspectral imaging detectors. The device would be used to sequentially choose the specific wavelength in the range of 3 to 5. Based on the method proposed that the directing vector of liquid crystal materials would be changed in an electric field applied over the electrodes of the device, the refractive index of the FP cavity filled by LC film could be changed electrically. Through the thin film matrix equation, we calculated the transmissivity of the infrared light incident upon the photosensitive plane directly, and then obtained the relationship among the transmissivity, the applied voltage signal, and the wavelength value selected. The most key features of the proposal approach was that the device will be composed of main very thin electrically refractive-index parts, which are two FP interferometers connected closely so as to accurately perform the choice of each single wavelength desired in the spectral range by the device developed.

Key words: Fabry-Perot interferometer; liquid crystal; single wavelength

CLC number: TN209 Document code: A Article ID: 1007-2276(2013)07-1853-05

中红外波段可调谐液晶法布里珀罗高光谱成像探测器

付安邦^{1,2,3}, 张怀东^{1,2,3}, 张新宇^{1,2,3}, 桑红石^{1,2}, 季安⁴, 谢长生^{1,2,3}

- (1. 多谱图像信息处理技术国防科技重点实验室, 湖北 武汉 430074;
2. 图像识别与人工智能研究所, 湖北 武汉 430074;
3. 武汉国家光电实验室, 湖北 武汉 430074; 4. 中国科学院半导体研究所, 北京 100083)

摘要: 提出了一种新颖的方法来研究电控可调谐液晶法布里珀罗高光谱成像探测器, 该设备将用于 3~5 μm 波段范围内连续挑选特定波长, 液晶指向矢会受到加在设备电极两端的电压产生的电场影响, 基于这个理论, 腔内的液晶折射率能够被电控。通过运用薄膜的矩阵传输公式, 计算了感光面上的红外透过率, 从而得到了透过率, 外加电压信号, 以及挑选波长之间的关系。最重要的理论是设备将由两个法布里珀罗干涉仪紧密连接起来, 分别受电控制, 从而达到准确的在波段范围挑选单一波长的目的。

关键词: 法布里-珀罗干涉仪; 液晶; 单波长

收稿日期: 2012-11-13; 修订日期: 2012-12-15

基金项目: 中国航天科技集团公司卫星应用研究院创新基金

作者简介: 付安邦(1990-), 男, 硕士生, 从事图像识别与人工智能方面的研究。Email: shabangsky@163.com

导师简介: 张新宇(1966-), 男, 教授, 博士, 主要从事微纳光电器件的制作方面的研究。Email: x_yzhang@yahoo.com

0 Introduction

In recent years, considerable efforts have focused on the development of interferometer technology using liquid crystal materials driven and controlled electrically. Two main methods including Micro-Electro-Mechanical Systems (MEMS) technology for changing the distance between two mirrors and electrically tunable liquid crystal technology^[1], have been used in the FP interferometer for choosing specific wavelength. Among them, MEMS structure has been proved to be useful for selecting specific wavelength by changing the depth of the FP cavity, thus the wavelength of the transmitted light can be changed^[2]. To the liquid crystal Fabry-Perot(LC-FP) interferometer, LC materials are filled into a FP cavity with a fixed thickness, and then the index of refraction of liquid crystal is varied electronically. Consequently, the structure can be used as a spectral imaging component that can be electronically controlled^[3-4].

Compared with the MEMS structure, the MEMS Fabry-Perot(MEMS-FP) structure has to adjust the depth of the FP cavity, so the LC-FP without mechanical movement of the mirrors demonstrates several advantages. First, the LC-FP has high stability, and the structure is only controlled by voltage so that the stability of the device can be ensured. Second, the fabrication of MEMS-FP is more complicated than that of LC-FP and it is difficult to make large area MEMS-FP arrays^[5].

This paper demonstrates the basic structure of the device model. Through sufficient calculations and simulations, the theoretical results provide a solid device design foundation for producing the future device. The model combines merit of each LC-FP structure, and thus the transmitted wavelength from the device is only unique and can be tunable.

1 Methodology and approach

1.1 Principle of FP interferometer

The main structure of the device is the FP

interferometer, so the principle of the FP interferometer is most important. The relationship between the I_i (the intensity of incident light) and the I_t (the intensity of transmitted light) can be characterized using the Airy equation^[6-8].

$$I_t = \frac{T^2}{(1-R)^2 + 4R \sin^2(\delta/2)} I_i \quad (1)$$

$$\delta = 4\pi n d \cos \theta / \lambda \quad (2)$$

In the equation (1) and (2), T reflects the transmissivity of the electrode, R represents the reflectivity of the electrode, δ represents the phase difference between consecutive reflection rays, n is the refractive index of the LC material, d is the depth of the FP cavity. From the equation, if the $\delta=0^\circ$, the I_t gets the maximum value. When $\delta=0^\circ$, we can obtain the equation(3).

$$2nd = k\lambda_k \quad (3)$$

where λ_k is the wavelength at k -level transmittance peak, the distance between contiguous transmittance peaks can be deduced as the equation (4) shows.

$$FSR = \lambda_k - \lambda_{k+1} = 2nd/k - 2nd/(k+1) =$$

$$2nd/k(k+1) = 2nd \left(\frac{\lambda_k}{2nd} \cdot \frac{\lambda_{k+1}}{2nd} \right) = \frac{\lambda_k \lambda_{k+1}}{2nd} \quad (4)$$

From the equation (4), we know if we want to change the value of the distance between contiguous transmittance peaks(FSR), you can adjust the n and d , as we use the LC-FP structure, so the n changes, then the FSR changes.

1.2 Method of liquid crystal

The directing vector of LC changes when the applied voltage changes, the refractive index of the LC material can be modulated by only controlling the voltage signal applied over the Al electrodes fabricated in LC-FP structures, the twisted angle θ (the angle away the parallel direction) changes when the FP cavity is under the control of the voltage. The effective refractive index of the LC can be described by the equation (5).

$$n_{\text{eff}} = n_o n_e / (n_o^2 \cos^2 \theta + n_e^2 \sin^2 \theta)^{1/2} \quad (5)$$

When no voltage is applied, the LC molecules are aligned parallel to the quartz substrates, the $n_{\text{eff}} = n_e$,

the voltage becomes strong, the n_{eff} turns down to n_0 . So when a light with many different wavelengths impacts the LC-FP, only some of the wavelengths can pass through, these wavelengths can be controlled. If we divide the LC layer to m parts, assume the refractive index of each part is n_k , we divide the LC into m levels, the total effective refractive index n of the structure can be calculated by the equation(6).

$$n_k = \sum_{k=m} n_k / m \quad (6)$$

In the simulation, we assume $m = 100$, if the applied voltage changes, the numerical solution of LC devices can be obtained by combining iterative finite-difference method and calculus of variations, we can obtain n_k at each level, so the total refractive index.

2 Simulations

The design of the device combines two LC-FP structures, the whole structure is showed in Fig.1. Figure 2 shows the overview of the device, Fig.3 shows the desired outlook of the device. The LC is in the middle of the substrates, the electrodes, the dielectric mirrors, the alignment films. As this device works in the range $3.0-5.0 \mu\text{m}$, the electrode and the dielectric mirror can be replaced by aluminum mirrors, the Al mirrors can be used as electrode and mirror in the working wavelength. From the Fig.4, we can see the device contains two LC-FP structure, assume the top structure is structure 1, the bottom structure is structure 2, one of the substrates is shared. The depth of the two structures is different, the structure 1 is $15.3 \mu\text{m}$, the structure 2 is $9.3 \mu\text{m}$. When the applied voltages are both at 5 V, the transmissivity are in the Fig.4. The figure shows that in the working wavelength, the transmissivity of the separate structure, as the depth is different, the number of transmittance peaks is different. If the applied voltage changes, we can see the transmittance peaks move. Figure 5 shows that when the applied voltage changes from 1-10 V, the transmittance peaks move to the left, and in the range 2-5 V, the result obviously changes.

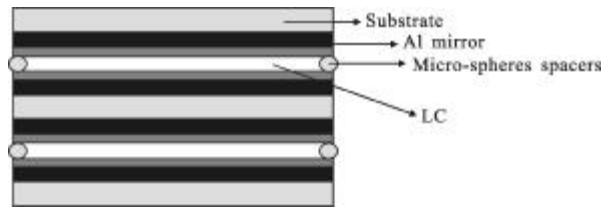


Fig.1 Structure of LC-FP interferometer

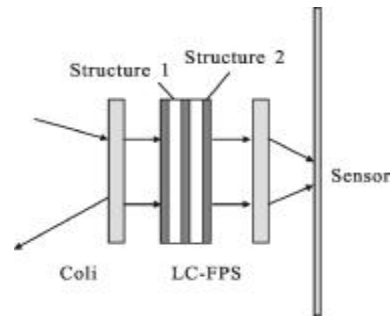


Fig.2 Overview of device

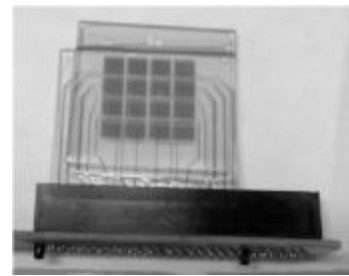


Fig.3 Desired outlook of the device

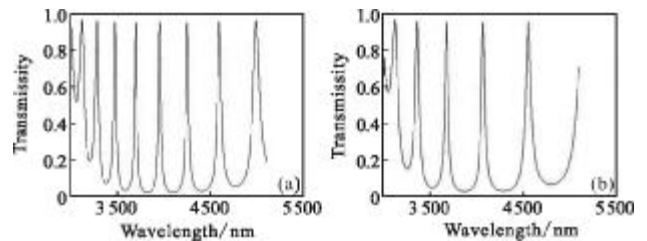


Fig.4 Transmissivity of two structures

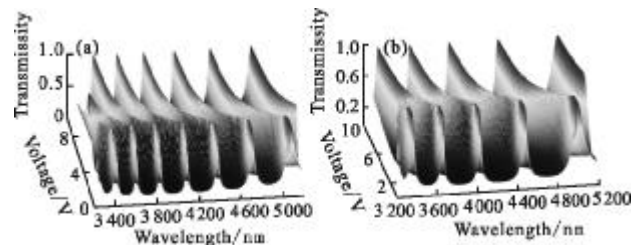


Fig.5 Applied voltage(x-axis), wavelength(y-axis), relationship between transmissivity(z-axis)

Then we let the two structures combine, as the voltage which apply to the electrode is separated, two

controlling voltage devices are needed. When the two applied voltages adjust independently, the transmitted intensity and the transmittance peaks change both. The total result is the product of the two independent transmissivity. From Fig.4 we can discover that in the range 3.0–5.0 μm , there are several transmittance peaks, if the two structures combine, with the changing voltage signals, we can obtain only one peak at the specific wavelength.

Assume the two voltages are U_1, U_2 , different U_1 and U_2 lend to different results. When $U_1=2\text{ V}$, $U_2=4.5\text{ V}$, the result can be seen in Fig.6. As the result shows that at 3 420 nm, transmitted light reaches a maximum transmittance, the FWHM(full width at half maximum) is 20 nm. When $U_1=2.5\text{ V}$, $U_2=4.5\text{ V}$, the result can be seen in the Fig.7. As the result shows that at 3 720 nm, the transmitted light reaches a maximum transmittance, the FWHM is 20 nm.

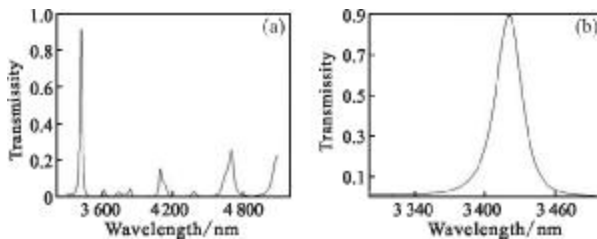


Fig.6 Transmittance peak at 3 420 nm

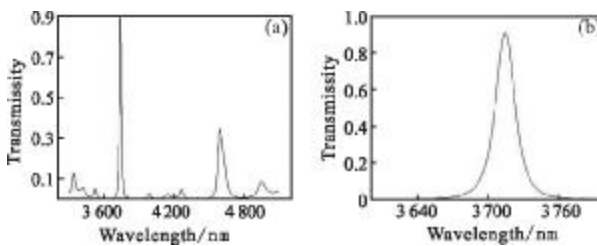


Fig.7 Transmittance peak at 3 720 nm

When the applied voltage is different, the phenomenon have greatly difference. If we want to obtain the right wavelength, we let one voltage remain unchanged, the other one changes from 1 to 10 V, we can see the simulation in Fig.8, Fig.9 separately. Figure 8 shows that U_1 remains unchanged, we change U_2 from 1 to 10V, the peaks change as U_2 changes. Figure 9 shows that when U_2 remains unchanged, we change U_1 from 1 to 10V, the peaks change as U_2 changes. In fact, when

the voltage changes as 0.1 V, the spectral can change obviously. From the result of the simulation, we can obtain almost 30 transmittance peaks in the range of 3–5 μm . The intensity of the transmitted light can over 80%.

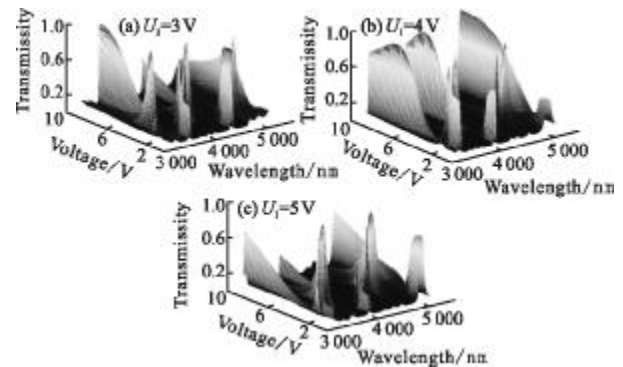


Fig.8 U_1 remains unchanged, the peaks change as U_2 changes

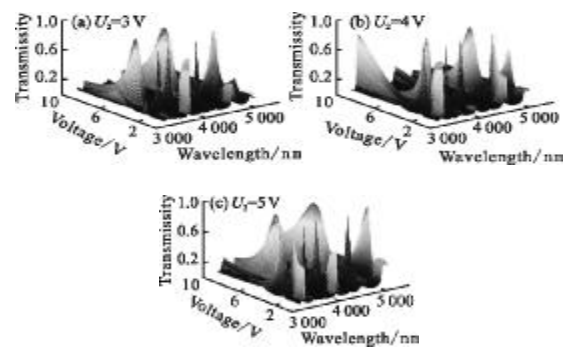


Fig.9 U_2 remains unchanged, the peaks change as the U_1 changes

3 Conclusion

In summary, we obtain a large number of simulations based on the basic model of the device which combines two LC-FP structures. By comparing the simulation of two structures separately and together, the two structures which connect closely demonstrate some advantages. The refractive index of the LC material can be modulated by only controlling the voltage signal applied over the Al electrodes fabricated in LC-FP structures. In the further work, we hope that the device is a 4×4 addressable planar array structure. Thus when the voltage that is applied over different cells, the FP array is changed separately, the wavelength of transmitted light can be chosen independently.

4 Acknowledgments

The authors are grateful to the Analytical and Testing Center of Huazhong University of Science & Technology for valuable help. This research was supported by the Key Fund of Wuhan National Laboratory for Optoelectronics (No. 0101187006), the National Natural Science Foundation of China (No. 61176052 and 60777003) and the Fundamental Research Funds for the Central Universities (No. 2011TS154).

References:

- [1] Katsuhiko Hirabayashi, Hiroyuki Tsuda, Takashi Kurokawa. Tunable liquid-crystal Fabry-Perot interferometer filter for Wavelength-Division Multiplexing Communication Systems[J]. *Journal of Lightwave Technology*, 1993, 11(12): 2033-2043.
- [2] Chen Polun, Lin Kuencherg, Chuang Weiching, et al. Analysis of a liquid crystal Fabry-Perot etalon filter: a novel model[J]. *IEEE Photonics Technology Letters*, 1997, 9: 467-469.
- [3] Stockley Jay E, Sharp Gary D, Kristina M Johnson, et al. Fabry-Perot etalon with polymer cholesteric liquid-crystal mirrors[J]. *Optics Letters*, 1999, 24(1): 55-57.
- [4] Lo Shihshou, Chen Chiichang. High finesse of optical filter by a set Fabry-Perot cavity [J]. *J Opt Soc Am B*, 2007, 24(8): 1853-1856.
- [5] Norbert Neumann, Martin Ebermann, Steffen Kurth, et al. Tunable infrared detector with integrated micromachined Fabry-Perot filter [J]. *J Micro/Nanolith MEMS MOEMS*, 2008, 7(2): 021004-1-021004-9.
- [6] Liu K, Li H, Zhang X, et al. Smart hyperspectral imaging detection based on electrically tunable liquid-crystal Fabry-Perot microstructure array [C]//*SPIE*, 2009, 7457: 74570U-1-74570U-10.
- [7] Li H, Liu K, Zhang X, et al. Low voltage adaptive 128×128 element liquid crystal micro lens array with electric tunable focal length[C]//*SPIE*, 2009, 7414: 74140V-1-74140V-9.
- [8] Liu Kan, Li Hui, Zhang Xinyu, et al. Development and characterization of an electrically tunable liquid-crystal Fabry-Perot hyperspectral imaging device [J]. *Journal of Applied Remote Sensing*, 2011, 5: 053539-1-053539-15.